

## *Supplementary material*

# **Impact of the temperature-cloud phase relationship on the simulated Arctic warming during the last interglacial**

Nozomi Arima<sup>★1</sup>, Masakazu Yoshimori<sup>★1</sup>, Ayako Abe-Ouchi<sup>1</sup>, Ryouta O’ishi<sup>1</sup>, Wing-Le Chan<sup>1</sup>, Sam Sherriff-Tadano<sup>2</sup>, and Tomoo Ogura<sup>3</sup>

<sup>1</sup>Atmosphere and Ocean Research Institute, The University of Tokyo, Kashiwa, Japan

<sup>2</sup>University of Ryukyus, Okinawa, Japan

<sup>3</sup>National Institute for Environmental Studies, Tsukuba, Japan

★These authors contributed equally to this work.

10 Correspondence to: Masakazu Yoshimori (masakazu@aori.u-tokyo.ac.jp)

### **1 The average autoconversion rate of cloud particles**

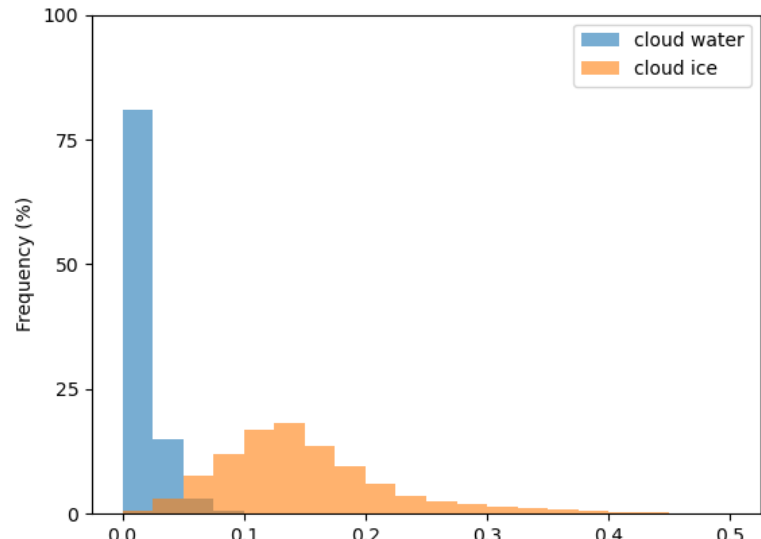
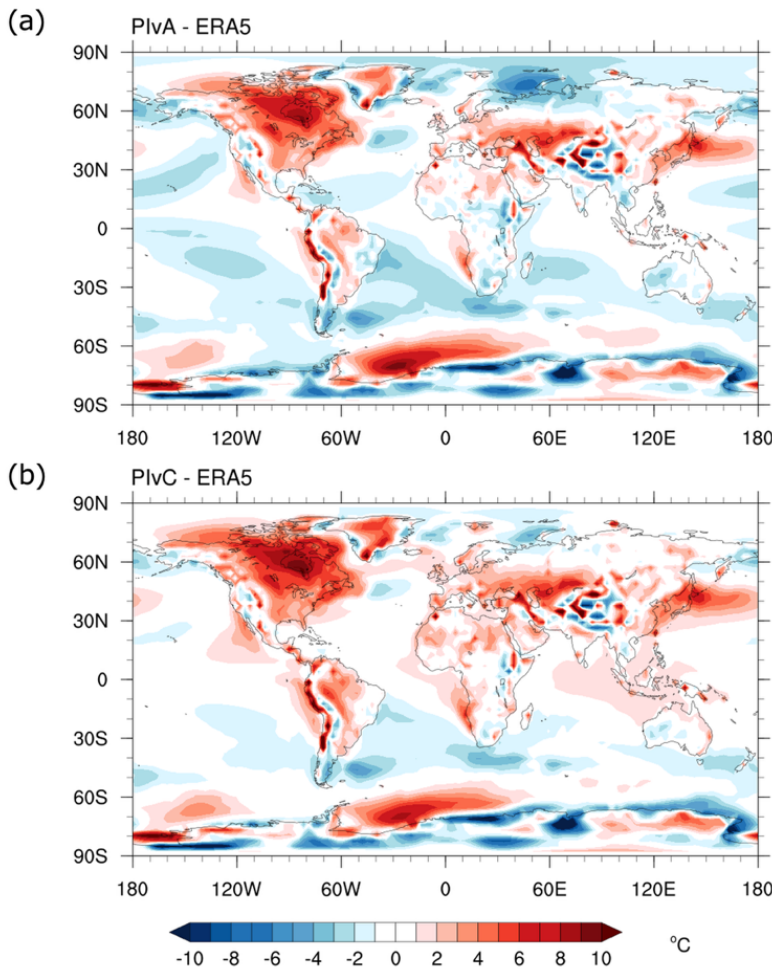


Figure S1: Histograms of the monthly mean autoconversion rate ( $-1/L \cdot dL/dt$ ) of cloud particles with  $L$  being the cloud liquid or solid water content for PIvA using MIROC4m-LPJ (see main text for the details). The data represent grid points below the 680 hPa level in the Arctic. The unit of the horizontal axis is (1/hour). The vertical axis is the fraction of the total number of grids. The figures for PIvC, LIGvA, and LIGvC are qualitatively similar and are therefore not shown.

## 2 Comparison with reanalysis data



20  
Figure S2: Difference in annual mean surface air temperature: (a) PIvA and ERA5 (Hersbach et al., 2020); and (b) PIvC and ERA5 (°C). ERA5 data represent average of 30 years from 1979 to 2008. Note that the comparison is crude as the PIvA and PIvC correspond to preindustrial conditions.

25 Data availability disclaimer: The ERA5 dataset was downloaded from the Copernicus Climate Change Service (C3S) Climate Data Store. Neither the European Commission nor ECMWF is responsible for any use that may be made of the Copernicus information or data it contains.

### 3 AOGCM results without dynamic vegetation feedback (MIROC4m)

30

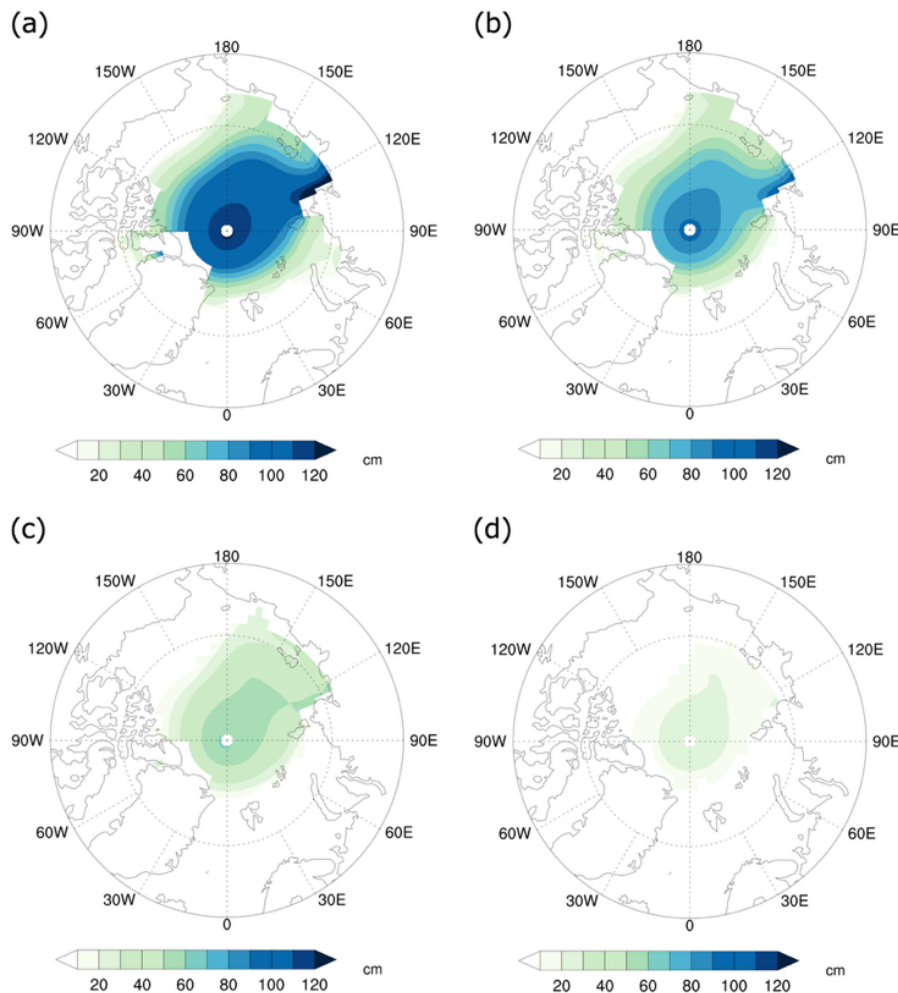
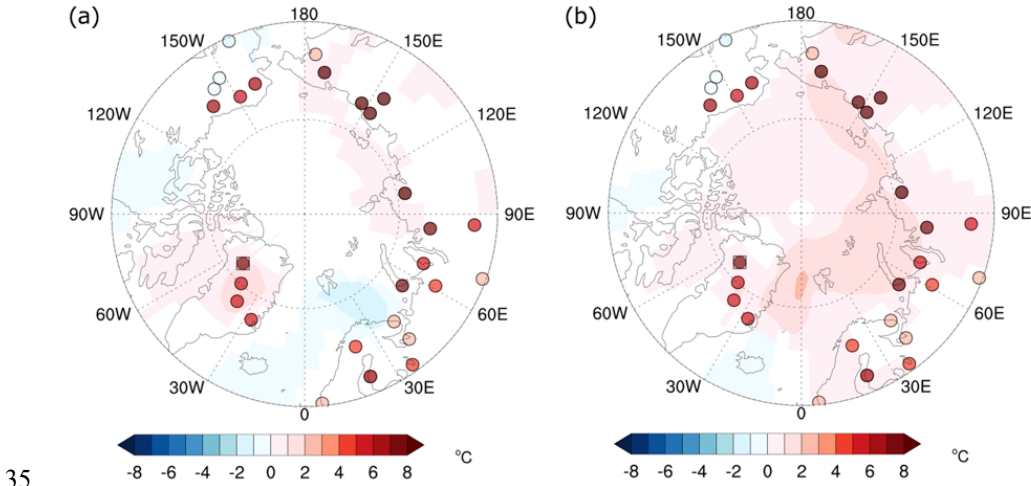
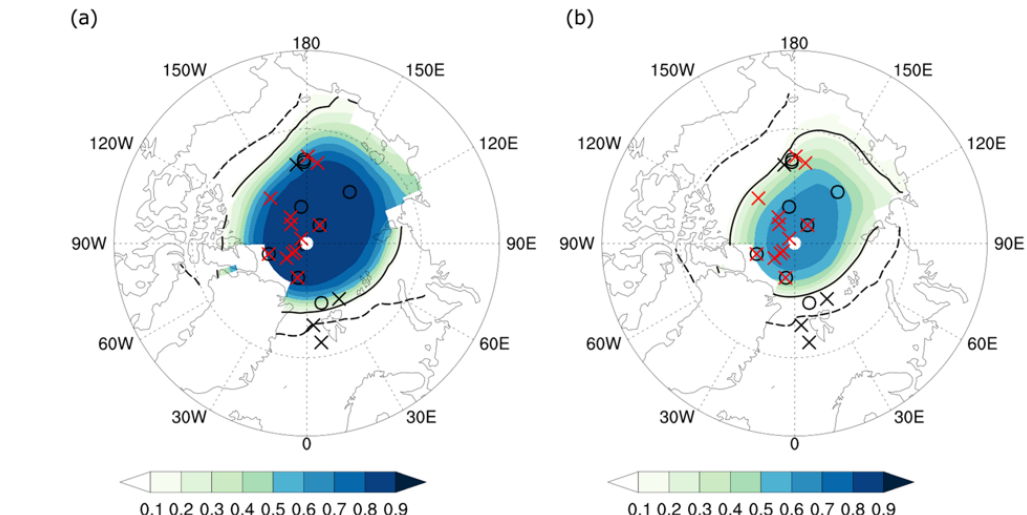


Figure S3: September sea-ice thickness (cm) in the Arctic: (a) PIIfA; (b) PIIfC; (c) LIGfA; and (d) LIGfC.



35 **Figure S4:** Comparison of simulation with proxies for the  $\Delta$ LIG annual mean SAT difference: (a)  $\Delta$ LIGvA (=LIGvA-PIvA); (b)  $\Delta$ LIGvC (=LIGvC-PIvC). Only grids where the difference is significant at the 5% level are colored, applying the Student's t-test for 100 samples from the last 100 years of each experiment. The circles are the proxies from Turney and Jones (2010), and the squares are the proxies from Capron et al. (2017).

40



45 **Figure S5:** September sea-ice concentration in the Arctic: (a) LIGfA; and (b) LIGfC. Black solid lines denote the simulated boundaries for the ice concentration of 0.15, while black dashed lines denote those in the corresponding preindustrial simulations. The year-round ice cover (circles) and summer ice-free conditions (crosses) suggested by proxies are also plotted: Black symbols for Kageyama et al. (2021) and red symbols for Vermassen et al. (2023).

## References

Capron, E., Govin, A., Feng, R., Otto-Bliesner, B. L., and Wolff, E. W.: Critical evaluation of climate syntheses to benchmark CMIP6/PMIP4 127 ka Last Interglacial simulations in the high-latitude regions, *Quaternary Science Reviews*, 168, 137-150, 2017.

Hersbach, H., Bell, B., Berrisford, P., Hirahara, S., Horányi, A., Muñoz-Sabater, J., Nicolas, J., Peubey, C., Radu, R., Schepers, D., Simmons, A., Soci, C., Abdalla, S., Abellán, X., Balsamo, G., Bechtold, P., Biavati, G., Bidlot, J., Bonavita, M., De Chiara, G., Dahlgren, P., Dee, D., Diamantakis, M., Dragani, R., Flemming, J., Forbes, R., Fuentes, M., Geer, A., Haimberger, L., Healy, S., Hogan, R. J., Hólm, E., Janisková, M., Keeley, S., Laloyaux, P., Lopez, P., Lupu, C., Radnoti, G., de Rosnay, P., Rozum, I., Vamborg, F., Villaume, S., and Thépaut, J. N.: The ERA5 global reanalysis, *Quarterly Journal of the Royal Meteorological Society*, 146, 1999-2049, 2020.

Kageyama, M., Sime, L. C., Sicard, M., Guarino, M.-V., de Vernal, A., Stein, R., Schroeder, D., Malmierca-Vallet, I., Abe-Ouchi, A., Bitz, C., Braconnot, P., Brady, E. C., Cao, J., Chamberlain, M. A., Feltham, D., Guo, C., LeGrande, A. N., Lohmann, G., Meissner, K. J., Menzel, L., Morozova, P., Nisancioğlu, K. H., Otto-Bliesner, B. L., O'Ishi, R., Ramos Buarque, S., Salas y Melia, D., Sherriff-Tadano, S., Stroeve, J., Shi, X., Sun, B., Tomas, R. A., Volodin, E., Yeung, N. K. H., Zhang, Q., Zhang, Z., Zheng, W., and Ziehn, T.: A multi-model CMIP6-PMIP4 study of Arctic sea ice at 127 ka: sea ice data compilation and model differences, *Climate of the Past*, 17, 37-62, 2021.

Turney, C. S. M. and Jones, R. T.: Does the Agulhas Current amplify global temperatures during super-interglacials?, *Journal of Quaternary Science*, 25, 839-843, 2010.

Vermassen, F., O'Regan, M., de Boer, A., Schenk, F., Razmjooei, M., West, G., Cronin, T. M., Jakobsson, M., and Coxall, H. K.: A seasonally ice-free Arctic Ocean during the Last Interglacial, *Nature Geoscience*, doi: 10.1038/s41561-023-01227-x, 2023.